

Observational Signatures of Black Holes: Spectral and Temporal Features of XTE J1550-564

Lev Titarchuk^{3,1}, & C.R. Shrader^{1,2}

ABSTRACT

The theoretical predictions of the converging inflow, or Bulk-Motion Comptonization model are discussed and some predictions are compared to X- and gamma-ray observations of the high-soft state of Galactic black hole candidate XTE J1550+564. The $\sim 10^2$ -Hz QPO phenomenon tends to be detected in the high-state at times when the bolometric luminosity surges and the hard-power-law spectral component is dominant. Furthermore, the power in these features increases with energy. We offer interpretation of this phenomenon, as oscillations of the innermost part of the accretion disk, which in turn supplies the seed photons for the converging inflow where the hard power-law is formed through Bulk Motion Comptonization (BMC). We further argue that the noted lack of coherence between intensity variations of the high-soft-state low and high energy bands is a natural consequence of our model, and that a natural explanation for the observed hard and soft lag phenomenon is offered. In addition, we address some criticisms of the BMC model supporting our claims with observational results.

Subject headings: accretion — black hole physics — binaries: close — radiation mechanisms: nonthermal — Compton and inverse Compton — relativity — stars: individual (XTE J1550+564, XTE J1118+480)

1. Introduction

It has long been known that accreting stellar-mass black holes (BH) in Galactic binaries exhibit a “bi-modal” spectral behavior - namely the so called high-soft and low-hard spectral states; see Liang (1998) for a recent review. High and low in this context refer to the

¹Laboratory for High-Energy Astrophysics, NASA Goddard Space Flight Center, Greenbelt, MD 20771, USA; shrader@grossc.gsfc.nasa.gov

²Universities Space Research Association, Lanham MD

³George Mason University/CEOSR; lev@lheapop.gsfc.nasa.gov; lev@xip.nrl.navy.mil

relative 2-10 keV luminosities in a given system, which is related to the rate at which mass accretion is taking place. An increase in the soft blackbody luminosity component leads to the appearance of the extended power law. An important observational fact is that this effect is seen as a persistent phenomenon only in BHCs, and thus it is apparently a *unique* black hole signature.

Although in Neutron star (NS) systems similar power law components are detected in the intermediate stages (Strickman, Barret 1999; Iaria et al. 2000; Di Salvo et al. 2000), they are of a transient nature, disappearing with the luminosity increase (Di Salvo et al.). The low-hard state spectral form on the other hand, has been seen in BH and NS binaries as well under certain condition. It was previously believed that the hard component in NS systems was associated with the low luminosity states of bursters (Barret & Grindlay 1995; Heindl & Smith 1998) when the soft component is suppressed.

It thus seems a reasonable assumption that the unique spectral signature of the soft state of BH binaries is directly tied to the black hole event horizon. This is the primary motivation for the Bulk Motion Comptonization Model (BMC) introduced in several previous papers, and recently applied with striking success to a substantial body of observational data. A complete theory of black hole accretion must, however, be also able to accommodate in a natural manner a growing number of empirical traits exhibited in the temporal domain. For example, it is now well established that black hole X-ray binaries exhibit quasi-periodic oscillation (QPO) phenomena in essentially three distinct frequency domains; low, ~ 0.1 Hz, intermediate ($\sim 1 - 10$ Hz) and high ($\sim 10^2$ Hz). It is likely that these are interrelated by some as yet unspecified underlying physics. The high-frequency QPOs seem to occur during periods of flaring, and when the spectra (although in the high-soft state) tend to be relatively hard, i.e. the proportional hard-power-law to thermal excess flux ratio is larger than usual. Furthermore, the QPO amplitudes increase with energy, that is there is a higher degree of modulation of the signal in the hard-power law than in the thermal excess component. In addition to the QPO phenomena, it has been noted by Nowak et al (2000) (also see Cui, Zhang, & Chen 2000) that measures of the coherence between the intensity variations in the hard power law and thermal components is negligible.

In this paper we present empirical evidence in both the temporal and spectral domains in support of our ideas on the converging inflow phenomenon and the BMC model. In section 2, we describe the main observational consequences of the Comptonization model for high-soft and low-hard states based on the presence of thermal and advection dominated (converging inflow) motions around the compact objects. We consider some empirical properties of accreting black holes in Section 3, highlighted by recent observations of XTE J1550-564. Interpretation within the context of our BMC model is presented. In section 4 discussion

of issues such as the reliability of obtaining the correct spectra from the deconvolution of time-varying, background dominated signals is discussed. We also investigate possible high-soft-state features such as Compton reflection and relativistically broadened line reported in the recent literature, and present physical parameter estimation (distance-to-mass ratio) for XTE J1550-56. In addition we consider the interrelation between spectral and temporal black hole properties, identifying further support of the converging-inflow hypothesis. Summary and conclusions are offered in section 5.

2. The Bulk-Motion Comptonization Model

2.1. An Overview and Synopsis of the Recent Literature

As noted, the specific spectral and timing features of the X-ray radiation characterizing the high-soft and low-hard states presumably provide insights into the underlying physical processes. The thermal Comptonization model (Sunyaev & Titarchuk 1980; Titarchuk 1994; Hua & Titarchuk 1995; Poutanen & Svensson 1996) quite well fits the low-hard state spectra with a typical electron temperature of $T_e \sim 60$ keV and optical depth $\tau \sim 1$ (Zdziarski 2000). These parameters seem to describe both galactic and extragalactic BH sources over the broad range of luminosities, characteristics of those objects; the energy spectral indices α and electron temperatures kT_e are consistently about 0.7 and 60 keV respectively. When the luminosity of the thermally radiating disk reaches a certain threshold, the power law steepens with the canonical value of $\alpha \approx 0.7$ changing to $\alpha \approx 1.5$. Laurent & Titarchuk (1999, see also Titarchuk, Lapidus & Muslimov 1998, hereafter TLM98) argued that this type of the spectral phase transition is a consequence of the bulk and thermal motions in a Compton cloud surrounding the black hole.

Sunyaev & Titarchuk (1978; 1980 hereafter ST80) first demonstrated, using an analytical Comptonization theory, that the observed spectrum of Cyg X-1 (Sunyaev & Trumper 1979) can be represented quite precisely by a thermal Comptonization spectral model. It was thus shown that X-ray radiation in the energy band from a few to several hundred keV is a result of the soft disk photons upscattering off thermal electrons. Chakrabarti & Titarchuk (1995 hereafter CT95) subsequently demonstrated through hydrodynamical calculations, a centrifugal-barrier shock region is formed in the region around compact objects ($10\text{-}20 R_s$) where the accreted matter releases its gravitational energy and heats that region to temperatures of 30-70 keV. In TLM98, the authors argued that any Keplerian motion in the disk has to pass through the centrifugal barrier (CB) region if the inner disk boundary rotates with a sub-Keplerian velocity. The CB location depends on the effective Reynold's number which, they point out, leads to CB oscillations which can in turn lead to an observable QPO

signature.

The presence of the bulk motion in addition to thermal motion in the Compton cloud is an unavoidable consequence of the gravitational attraction by the central source. Blandford & Payne (1981) were first to address the issue of bulk-motion effects on the emergent spectra of accreting black holes by formulating and solving the bulk motion problem in the simplified context of a nonrelativistic Fokker-Planck treatment. They considered a semi-infinite converging inflow atmosphere without taking into account any effects of General Relativity. The first realization that the high-soft state black hole spectra might be related to Bulk Motion Comptonization was put forth by Titarchuk, Mastichiadis & Kylafis [1996 and in the extended version in (1997), hereafter TMK].

Zane et al. (1996) have elaborated the numerical method of characteristic for the solution of general relativistic kinetic (GRK) equation for the bulk inflow atmosphere. Subsequently, Titarchuk & Zannias (1998 hereafter TZ98) solved semi-analytically the relativistic kinetic equation for a finite converging inflow atmosphere using the separation variables method but they neglected the recoil effect in photon-electron interactions. Laurent & Titarchuk (1999) reproduced TZ98's results through Monte Carlo simulations and they calculated the overall spectrum taking into account all effects of the photon-electron interactions and the Special and General Relativity Theory.

Recently, Papathanassiou & Psaltis (2001, hereafter PP01) presented calculations of the resulting spectrum of the bulk-motion atmosphere. They solved numerically the general-relativistic kinetic (GRK) equation in the steady-state Schwarzschild spacetime, neglecting the recoil effect in photon-electron interactions. They demonstrated that power-law spectra result from multiple scatterings, similar in some regards to thermal Comptonization.

PP01 conclude that “the photons emerging from the accretion flow with high energies do not carry any signatures of regions of high velocities or space time”. However, their calculations do not allow them to make this strong statement because they neglect the recoil effect. The estimate of the mean electron energy is determined by the position of the high energy cutoff in the spectrum. It is the same as in the thermal Comptonization case (see for example ST80). The spectral index itself which is a real outcome of PP01 calculations does not allow for estimates of the average electron energy. *In TZ98 and PP01, following separate and independent approaches to solving the same kinetic equation, both sets of authors elaborate the necessary properties of the Bulk motion inflow in Schwarzschild space time: spectral indices which converges to the asymptotics value of $\simeq 1.7$, and a hard-photon source distribution confined to ~ 3 Schwarzschild radii.* For additional details, we refer the reader to the references contained in in TMK97, PP01 and Psaltis (2001).

We also note recent work by Reig et al (2001), who have considered the possibility that rotational motion of electrons in the disk upscatter photons to produce the high-energy power law. They are similarly able to reproduce the basic high-energy continuum properties, provided that the disk vertical optical depth exceeds some threshold value near the innermost Keplerian orbit.

2.2. Predictions of Observable Black-Hole Properties

Most of the spectral and temporal properties predicted theoretically by the BMC model can in principle be verified by observations. They are: (i) the specific high-energy spectral index, $\alpha \simeq 1.75$ in the limits of high accretion rates and low electron temperatures of order 1 keV and less; (ii) the presence of a high energy turnover, at energies between 300-500 keV; (iii) QPOs detected as oscillations of the hard power law component formed in the same inner-disk vicinity through bulk motion upscattering. These are due to a hard photon-source distribution with a strong maximum about $(1.5-1.8) R_s$ (TZ98, Fig. 3, see also Laurent & Titarchuk 2001) which result from the strong photon bending and Doppler effects in the immediate vicinity of a black hole. The contribution to the total disk flux from the innermost region is generally small, hence these oscillations would not be detected. (iv) a lack of discernible coherence between the temporal signals of the high-state soft-thermal emission, emanating from a relatively large region, and the hard-power-law emission emanating from a compact region, and illuminated by a relatively small fraction of the overall thermal emission, and finally, (v) an increase in this coherence measure as the source transitions to the low-hard state.

2.3. Emergent Thermal Spectrum: The Hardening Factor

Empirical support of the BMC model, based on numerous high-soft-state BHC observations, has been presented in papers by Shrader & Titarchuk (1998, hereafter ShT98), Borozdin et al.(1999, hereafter BOR99) and Shrader & Titarchuk (1999, hereafter ShT99). In BOR99 and ShT99 it was shown through high quality fits of the BMC model to the observed spectra, that the soft component can be extracted with a high degree of accuracy. The emergent soft flux component depends strongly on BH mass, distance and a color correction or "hardening factor" T_h , which is the ratio of the effective to observed blackbody color temperature (see BOR99). Because the mass and distance are known to a high degree of accuracy for GRO J1655-40, it was possible to determine $T_h \approx 2.6$.

Recently Zhang et al. (2000) and Merloni, Fabian & Ross (2000) have also pointed out the importance of the hardening factor determination. There is an essential difference between the BOR99 empirical determination and the Zhang et al (2000) determination. In BOR99 the authors extracted the blackbody-like component from the high-soft spectrum of GRO J1655-40 using BMC's model. The quality of fit was very high with χ^2 per degree of freedom of order unity (see BOR99, Table 3 and Fig. 1). They found that the presence of a blackbody-like spectral component was consistent with the data. Then, assuming the thermal component emanates from the disk, the Shakura-Sunyaev 1973 model (hereafter SS73) is used to determine $T_h \simeq 2.6$. Recently, the value $T_h = 2.6$ for GRO J1655-40 was independently confirmed by Ebisawa et al. (2001).

In contrast with our determination Zhang et al. (2000) assumed that the disk component is embedded in a Comptonizing "haze", and is thus viewed through this medium. The hardening factor they derive is due then to upscattering of the disk soft photons in this medium, and it thus depends strongly on the optical depth and temperature (see Sunyaev & Titarchuk 1980). This being the case, the hardening factor can have any of a wide range of values (Zhang et al. found that $T_h = 3 - 6$). We concur that at times the "weather" in GRO J1655 may be such that the disk is covered by this relatively hot haze and additional spectral components may be needed to fit the data (see BOR99). But very often the effective emission area of the disk is directly observable and its intrinsic properties can thus be determined.

Merloni et al. (2000), using the numerical calculations of the disk spectral formation, confirm that the hardening factor can be noticeably higher than 1.7 which is widely assumed in the literature following Shimura & Takahara (1995). Furthermore they found (see Table 1 of their paper) that with certain combinations of model parameters the hard color factor can be very close to the empirically determined value $T_h = 2.6$. It is worth noting that the theoretically determined value of T_h is very sensitive to choice of model parameters, hence making it very difficult to use for BH mass determination. Given the large uncertainty in the α -parameter for realistic black-hole accretion disks, and because T_h changes drastically when α approaches unity [which can be the case at least for disks in NS binaries (Titarchuk & Osherovich 1999)], we have opted to proceed using our empirically determined value.

3. THE EMPIRICAL PICTURE

3.1. High-Energy Spectral Evolution

To illustrate some of these ideas we present our recent analysis of the X-ray nova XTE J1550-564 (e.g. Remillard et al 1999; Sobczak et al. 1999) which was observed by RXTE

and CGRO. This analysis is based on data obtained by the CGRO OSSE and BATSE instruments, and primarily, the RXTE PCA and HEXTE instruments.

The basic BMC model features can be seen in the context of an evolving source, in this case for XTE J1550-564 during the March 1999 time frame. The composite hard-soft X-ray light curve (Figure 1) illustrates roughly the evolution of that particular event—its rather gradual linear decay from about 2.5 to 2 Crab, followed by an exponential decay in the 2-10 keV band, with more erratic flaring behavior in the BATSE 20-100 keV band.

The spectra illustrated in Figure 2, derived from the RXTE observations of about TJD 11220 (where TJD=JD-2450000), represent the *extreme high soft-state* in XTE J1550- 564. The flux is completely dominated by thermal emission, with a characteristic temperature of $kT \simeq 1$ keV. The mass-accretion rate is high, as indicated by the $\simeq 2.5$ Crab flux (2-10 keV), and we speculate that the geometrical configuration of the thermal source expands due to viscous angular momentum loss in the inner disk. In the extreme case, only a small fraction of the thermal photons illuminate the bulk-in-flow site. Hard photons are further suppressed due to Compton down-scattering by the thermal plasma. As the accretion surge subsides, the situation moderates. This is reflected in the de-convolved spectra; the hard power-law component is barely discernible in the upper panel, and then slightly more pronounced in the lower panel. The parameters of the fit (panels a and b): $(T, \alpha, f) = (0.9, 3.7, 0.02)$ and $(0.9, 2.6, 0.06)$, where T is the temperature of the injected soft photons, α is the energy spectral index and f is the illumination factor.

As the mass-accretion further decreases and the system stabilizes, the hard X-ray flux increases in proportion to the thermal source. The resulting spectral form is the characteristic black-hole *high-soft state* spectrum, illustrated in two stages of evolution here. In the spectrum illustrated in panel (c), which is derived from RXTE PCA and HEXTE observations on TJD 11236, the hard power law is becoming more prominent. This is also evident in the upturn in the BATSE Light Curve. The next spectrum of the sequence, (d), is a composite from XTE and OSSE covering about 3-300 keV. The OSSE integration spans TJD 11253-11260. The hard power law is now very prominent out to ~ 200 keV where it becomes noise limited. This is reflected in the evolution in our inferred parameters, $(T, \alpha, f) = (0.9, 1.6, 0.11)$, that is the illumination fraction has now increased. It must be noted however, that the OSSE spectrum presented here represents an integration over the 1-week viewing period, whereas the RXTE soft X-ray spectra are typically $\sim 10^3$ s “snapshots”. This more than two orders of magnitude difference in the integration time for the RXTE/PCA and OSSE bands clearly makes problematic the identification of a high-energy spectral cutoff. Such a feature cannot be reliably established, primarily due to the noise-limited nature of the high-energy, but additionally because of the drastically different integration times of two these instruments

(in this particular case, the net background subtracted count-rate for the coarsely binned 400-650 keV interval is in fact negative by about 1σ). The long time integrations are unavoidable for the high energy part of spectra because of the very steep power law shape. But from the other hand they are problematic for the high-soft state, where any changes in the illumination geometry or mass accretion rate (of any sub-Keplerian or Keplerian portions of the flow) may lead to the drastic spectral changes.

As the outburst continues to evolve (Figure 2e & f), the luminosity of the thermal source decreases. The ambient plasma cloud can no longer be efficiently Compton cooled, and the thermal luminosity is thus further diminished by scattering. The resulting decrease in the thermal excess is clearly seen in this sequence of de-convolved spectra (in either case, a detection is made only up to 20 keV). This change is quantitatively reflected in the derived parameters: T decreases (0.75 to 0.34 keV), and f , which recall is related to the illumination parameter of the bulk-motion in fall, increases (0.2 to 0.31), although the power-law index is still consistent with the high-soft-state spectral form.

3.2. Spectral Characteristics Associated with QPO Behavior

In Figure 3, we show how continuum models derived through fits to BH X-ray nova XTE J15550-564 (panel a) and 4U 1630-47 (panel b). For XTE J15550-564 data from the two epochs; October 1998 (solid curve), when 185-Hz QPOs were reported (e.g. Remillard et al. 1999); and March 1999 when no prominent high-frequency QPOs are present. The October 1998 case represents a higher luminosity state than March 1999. The spectra are scaled for illustrative purposes. It is worth noting the dramatic difference in the proportional luminosity in the soft-to-hard components for the two cases. This is reflected in the inferred values of the f parameters, 0.04 and 0.6 for the two cases. 4U 1630-47 provides another, albeit less dramatic example (panel b).

We interpret this as being due to an enhanced illumination of the converging inflow site, $1 - 4 R_S$ for the hard/QPO case, which we conjecture results from a pile up of the material – i.e. the formation of a standing wave – in the inner disk region (TLM). This is also reflected in the larger parameter f , the BMC illumination factor, of our model (ShT98-99). We consider the *luminosity and spectral dependence, specifically the f -dependence, of the presence (absence) of the QPO as an additional support for the BMC model.*

3.3. Mass-distance estimate for XTE J1550-564

We have previously developed and presented a method for physical parameter estimation based the derived BMC model parameters (ShT99; see also BOR99). The basic idea is to infer the effective soft-emission region area in terms of the distance (typically unknown) and the previously mentioned hardening factor. The observable surface area can then be applied to a determination of the black-hole mass in terms of a specific disk model, typically that of SS73 with modification to treat electron scattering.

Applying our method to XTE J1550-564, we obtain the distance to mass ratio $d/m = 0.042 \pm 0.004$, where m in solar units and d is in units of 10 kps. A $\cos(i) = 0.5$ as a cosine of the inclination angle and the hardening factor $T_h = 2.6$ has been assumed in this calculation. This suggests a large black-hole mass, perhaps $m \simeq 10 - 15$ if the source is in the 5-kpc distance range. The distance is unknown for this source, but given the large column density $N_H = 2 \times 10^{22}$ it is probably more than a few kpc. We further note that for $d = 5$ kpc and our corresponding mass estimate, the source would have been radiating in the 5-7% L_{Edd} range during early March 1999 when the 2-10 keV flux was in the 2-2.5 Crab. However, given the apparently large mass accretion rate 10-15% L_{Edd} is more plausible and the distance may well be in the 7 – 8 kpc range calling for a larger BH mass.

4. Discussion

4.1. Spectral/Temporal Connections in BH Binaries

There are roughly speaking three “types” of QPO behavior seen in Galactic black hole binaries; ($\sim .1, 10, 100$) Hz. The latter 2 seem to be associated with “power law-dominant” high-soft states (e.g. Remillard. et al 1999; Cui et al 1997). The high-frequency cases are also luminosity dependent – they tend to be associated with luminosity surges – perhaps for the same reasons that kilohertz QPOs in neutron star sources are associated with high luminosity states of those objects. The high-frequency QPO amplitude is also seen to increase with energy [see e.g. Morgan et al (1997); Cui et al (2000)]. In our interpretation, this is because the high-energy photons are produced in a more compact region – i.e. the converging inflow site – than the low-energy ones which are produced in the inner-disk annuli. Another empirical trend that has emerged is that the break frequency, ν_b , of the power density spectra (PDS) increases with the photon energy (Belloni et al. 1997, Homan et al. 2000). Titarchuk & Osherovich (1999) have shown that the break frequency ν_b is related to the size of the emission region. This is because ν_b is inversely related to the emission area viscous time t_b . Thus smaller values of t_b imply smaller emission areas for a given energy band. This

is precisely the case for Bulk Motion Comptonization; harder photons are produced in the deeper layers of the converging inflow atmosphere.

We should also note that the coherence between low and high energies, e.g. between $\sim 2\text{--}5$ keV and > 6 keV, is small, in the soft-high state but it increases when the soft-to-hard state transition occurs (Cui et al. 1997; Nowak et al. 2000). In the framework of the BMC model, only the innermost part of the disk, of order a few R_S , provides the seed photons for the Bulk motion Comptonization and thus for hard photon production. The low degree of coherence between intensity fluctuations of the low-energy disk photons ($\sim 2\text{--}5$ keV), which come from much larger disk area of order $\pi[(10 - 15)R_S]^2$, with that of the high energy photons formed in the compact converging inflow region of order $\pi(3R_S)^2$ arises naturally. However the coherence is expected to increase for the soft-hard transition because the Comptonization region becomes larger and ultimately it completely covers the seed-photon area of the disk.

Each of these trends is *difficult to explain in context of “standard” disk plus coronae models*. They can in principle be reproduced by invoking additional parameter, such as a radial temperature gradient in the corona (e.g. Nobili et al. 2000; Lehr, Wagoner, & Wilms 2000), or by more elaborate geometrical and dynamical configurations (e.g. Boettcher & Liang 2000). However, we assert that *they are explained naturally and self consistently if the hard flux emanates from a compact region*. In this case, the: (i). high-frequency inner-disk oscillations are expected to be preferentially scattered, since only this small fraction of the thermal source illuminates CI region, (ii). higher energy photons are produced closer to the BH horizon (where the velocity is closer to the speed of light), and thus the compactness of the emission region increases with the energy, (iii). high luminosity is consistent with “pile up” in accretion flow.

4.2. Hard and Soft Phase Lags

Additional important information related to the X-ray spectral-energy distribution can be extracted from the time lags between different energy bands. While hard lags have been observed for several sources, soft phase lags have been found in some cases as well (e.g. Reig et al. 2000). In addition, there have been suggestions of separate harmonic components of given feature having lags of the opposite signs [e.g. Tomsick & Kaaret (2000) studied the QPO properties of GRS 1915+105 where both negative (soft) phase lags and positive (hard) lags were detected]. However, *it is natural to expect the positive time lags in the case of the thermal Comptonization. In the case of bulk-motion Comptonization, both negative and positive time lags are anticipated*. In the thermal Comptonization case, the primary soft

photons gain energy in process of scattering off hot electrons; thus the hard photons spend more time in the cloud than the soft ones. There is then a one-to-one correspondence between the photon energy and the photon travel time in the cloud. But this is not the case for bulk-motion Comptonization where soft disk photons at first gain energy in the deep layers of the converging inflow, and then in their subsequent path towards the observer lose energy in the relatively cold outer atmosphere. If the overall optical depth of the converging inflow atmosphere (or the mass accretion rate) is near unity, we would detect only the positive lags as in the thermal Comptonization case, because relatively few photons would lose energy in escaping. But with an increase of the optical depth, the soft lags appear because more hard photons lose their energy in the cold outer layers. There is a piling up effect at low energies due to the recoil effect (see ST80). A significant portion of the low-energy photon distribution, particularly at energies of order 2-5 keV, results from this piling up effect. The low-energy photons spend more time in the matter than the higher-energy photons because since they undergo additional scatterings from cold electrons of the outer regions.

In fact, for unsaturated Comptonization the spectral formation is mostly due to the Doppler effect but in the saturated case it is equally determined by recoil and the Doppler effects (see e.g. ST80 and figures of spectra there). For thermal Comptonization the relative change of energy $\Delta E/E = (4kT_e - E)/m_e c^2$. In the unsaturated case, the photon energy E , on average, is less than $4kT_e$ and thus most of the photons gain energy and the soft photons are led by the hard ones and thus the hard lags occur due to Comptonization. But in the saturated case when the Comptonization parameter is very high, i.e. when the product of $4kT_e/m_e c^2$ and τ^2 is greater than one, a significant fraction of the hard photons lose energy trying to thermalize to the average electron energy, kT_e . In this case there is a distribution of soft and hard lags as a result of Comptonization. Some of hard photons are followed by the soft ones.

A very similar situation is realized for the Bulk Comptonization where the temperature of the electrons should be replaced by $m_e v_b^2/3$ (TMK97, appendix D). Because in the outer part of the converging inflow atmosphere ($r > 5r_s$) $m_e v_b^2/3 = m_e c^2 (r_s/r)/3$ less than 30 keV the hard photons with energies more than 30 keV readily lose their energies and consequently the hard photons can be followed by the photons with energies less than 30 keV.

Because the hard state is characterized by the thermal Comptonization spectra we expect the hard lags in the hard state and *we expect the soft lags in the high-soft states characterized by high f values* (i.e. power-law dominated). Hard lags would be more likely to occur in high-soft states with lower f values. Laurent & Titarchuk (2001) present the extensive calculations of the distribution of time lags in the framework of the BMC model.

4.3. Additional Spectral Components

We also note that we have not included additional continuum features such as Compton reflection in our high-soft state analysis (e.g. Tomsick et al. 1999; Zdziarski, 2000; Gierlinski et al. 1999). While it may always be possible to improve the chi-square statistic through the introduction of additional parameters, our goal is to extract physical information invoking a minimal parameter space. Furthermore, the aforementioned analyses were motivated by the presence of significant residuals to additive continuum models (typically blackbody or multi-color disk plus power law). In our fitting however, we have not generally been so compelled. For example, for the GRO J1655-40 high-soft state covered by the TJD 10322-10328 OSSE observation we obtain a 3-parameter fit with a reduced chi-square statistic of $\chi^2_\nu \simeq 0.6$. This compares favorably to other efforts in the literature where more complex models are invoked. For example, a $\chi^2_\nu \simeq 0.7$ result was obtained by Tomsick et al (1999) by invoking a 8-parameter model including Compton reflection characterized by a 26% covering factor. The difference may have to do with the effects of applying an additive model as opposed to a self-consistently derived model to the instrumental response (Figure 4).

4.4. Extent of the High-Energy Power Law

Another issue regards the high-energy extent of the hard power law. As noted, the BMC model predicts a turnover of this power law below the electron rest-mass energy due to Compton recoil effects, relativistic bending of photon trajectories and gravitational redshift. There have been claims in the literature of detections to as high as 700 keV, however, what is generally presented is the high-energy extension of a power-law *fit* to the data, which is in fact dominated by the higher signal-to-noise detector count rates at lower energies. The problem is that the source count rates above ~ 500 keV are typically a fraction of a percent of the background count rates, and the long integration times required lead to systematic uncertainties which are hard to characterize. The first, and still the most notable case has been GRO J1655-40 (e.g. Grove et al 1997; Grove et al. 1998; Tomsick et al 1999). Referring to our analysis of GRO J1655-40 from the preceding section, a coarse binning of the data leads to a statistical significance of $\sim 3.5\text{-}\sigma$ in the 475-600 keV spectral range. To better address this issue we have analyzed 14 spectra from 6 Galactic BH binaries observed with OSSE during the CGRO mission. The resulting statistical distribution of detection significance for the $\simeq 450 - 750$ keV band is illustrated in Figure 5. Although, there is an apparent positive asymmetry relative to the overlaid Gaussian curve (which represents random statistical fluctuation about a zero mean), the results seem less than compelling, given the likely predominance of systematic uncertainties in this spectral domain.

We further note that while we have made a specific prediction regarding the high-energy extent of the BMC-produced high-energy power law, we are not ruling out the possibility of higher-energy gamma-ray emission from some other process.

The recent claim by Zdziarski et al. (2001) regarding the observational evidence of the nonthermal Comptonization and ruling out the bulk Comptonization for the high-soft state is based on the OSSE observation of the high-soft state in GRS 1915+105. The exposure time for these observations of $(2-7) \times 10^5$ s is incomparable with the dynamical time scale of the X-ray emission region of order of 10^3 s determined by the subKeplerian component. One should expect variability of the spectral index of the emergent spectrum within one hour or less. Furthermore, Focke et al. (1997) analyzed RXTE observations of Cyg X-1 in the soft state. They claimed significant variations of the hard tail photon index occurring in minute time scales. Thus it is very problematic to restore the true spectral shape (particularly the high energy turnover) using the data with the exposure time of order of a few times of 10^5 seconds when the real count rate from the source is washed out and additionally distorted by the high level X-ray background.

4.5. Sub-Keplerian Flows

CT95 first argued that two flows (subKeplerian and Keplerian) are always present in the binaries. Now this prediction is confirmed by the recent observation of a number of sources including XTE J1550-554 (Smith et al. 2001; Soria et al. 2001). The dynamical time scale of the propagation of the subKeplerian components towards the central object is very close to the free-fall time scale which is less than 10^3 s for a black hole of 10 solar masses.

4.6. Physical Parameter Extraction: Previous Approaches

We note that many efforts described in the literature have attempted to directly infer physical information through spectral deconvolutions based on specific disk models. The models are typically some variation of the SS73 formulation. We point out however, that the SS73 formulation invokes a dimensionless radial integration variable, and thus for example, *determinations of the inner disk radius in physical units are not valid.*

A full analytical presentation of the multi-color disk spectrum can be found in ShT99, equations 1 and 2. In this analysis, the spectrum is formulated as an integral over disk annuli with a lower limit expressed as the dimensionless inner radius, namely, $r_{\text{in}} = R_{\text{in}}/R_{\text{S}}$. Here R_{S} is the Schwarzschild radius. The temperature distribution in the SS73 formulation is described

by a function $f(r)$, where r is the dimensionless radius in Schwarzschild units (ShT99, equation 2). Mitsuda et al. (1984) [also see Makishima et al. (1986)] first suggested simplification of this integral (e.g. ShT99 equation 1) by ignoring the term $(r_{\text{in}}/r)^{1/2}$. *This simplification transforms the radial integration over the disk from dimensionless to dimensional units. Such a procedure is not mathematically correct.* It is nonetheless widely used in the community; it is for example, the formalism underlying the “diskbb” routine of the “XSPEC” package.

Despite this problem, in many instances in the literature of this field, values for the inner-disk radius are not only quoted in physical units to high degrees of precision, but the accompanying dialog often leaves the reader with the misleading impression that what is being presented is a *measurement*, rather than an *inferred parameter of a particular (and non-unique) spectral deconvolution*.

4.7. Global Disk Oscillations, Low Frequency QPOs and Mass Determination

The low frequency oscillations seen in hard state as well as soft, and at multiple wavelengths have been interpreted as the global disk mode (GDM) oscillations (Titarchuk & Osherovich, hereafter TO00). If the disk oscillates coherently as a single body, the observed frequencies should be seen in all wavelengths emitted by the extended disk, i.e. from optical to X-rays. The GDM frequency, of order 0.1 Hz for BH masses of order of 10-20 solar, is consistent with the observations (TO00). This lack of energy dependence, as well as the observed anticorrelation of the QPO frequency with the disk mass has been observed in XTE J1118+480 (Wood et al. 2000). The latter effect is also a natural consequence of GDM model, where QPO frequency anticorrelates with the disk mass which is believed to decrease during the soft-to-hard transition. The intensities and profiles of high-excitation optical/UV lines, believed to result from photoionization of the outer disk by X-irradiation, may also be modulated at the GDM frequency. This is a measurement which could in principle be made as a further test, and it also allows for a more precise estimates of the size and physical properties of the disk (Wood et al 2001).

The low-frequency QPOs, interpreted in the context of the GDM oscillations and the BMC model analysis provide two independent derivations of BH masses. This approach has been applied to derive the BH mass in LMC X-1 (TO00) which was earlier derived using the X-ray spectral method (ShT99). A similar procedure can be applied to XTE J1550-56, XTE J1859+227, and others. Recently McClintock et al. (2000); also see Wagner et al (2001) have independently confirmed earlier, more speculative results presented by Dubus et al. (2000) regarding the binary solution for XTE J1118+480. Those authors demonstrated through observations of the quiescent system that the velocity amplitude of

the dwarf secondary is $698 \pm 14 \text{ km/s}$ and the orbital period of the system is $0.17013 \pm 0.00010 \text{ d}$. The implied value of the mass function, $f(M) = 6.00 \pm 0.36$ solar masses, provides a hard lower limit on the mass of the compact primary that greatly exceeds the maximum allowed mass of a neutron star. Among the eleven dynamically established black-hole X-ray novae, the large mass function of XTE J1118+480 is rivaled only by V404 Cygni and XTE J1859+226. A large black hole mass, in XTE J1118+480 in fact, was predicted earlier by TO00 using the GDM frequency. The GDM leads to a BH mass estimate for XTE J1118+480 of $\sim 7M_{\odot}$ based on the $\sim 0.1 \text{ Hz}$ QPO frequency, in agreement with the optical observations by Wagner et al. (We note there is a typographical error in equation (14) of TO00 which should have $x_{\text{in}}^{-4/5}$ instead of $x_{\text{in}}^{-8/15}$.) We note that distance-to-mass determination method based on the BMC formalism (BOR99, ShT99 and section 4.5) could not be applied to this source since it observed only in the low-hard spectral state.

4.8. High - Frequency QPOs

As a synopsis of the QPO behavior in BH binaries it is worthwhile to note that sources such as XTE J1550-56, 4U 1630-47, XTE J1859+227 exhibit $\sim 10^2 \text{ Hz}$ QPO behavior only when high “ f ” values are seen in our analysis (f parameterizes the fractional illumination of the CI region; see BOR99). The intermediate case, i.e. $\sim 10 \text{ Hz}$ QPOs, are more ambiguous and the low-frequency ($\sim 10^{-1}$) QPOs seem to be energy independent, spanning the X-ray to near IR bands (Haswell et al. 2000; Wood et al 2000; Chaty et al 2000). Low-frequency QPOs are seen in low-hard and high-soft states but high-frequency cases only in high-soft states (Remillard et al 1999; Cui 1998). Thus, there is a apparently certain connection between different QPO regimes. The observations seem to be suggesting that the presence of the low frequencies is not associated with spectral state transitions, whereas high frequencies appear only in the high-soft state, albeit an extreme manifestation (hard-power-law dominated) of that state. It is worth noting that in GRS 1915+105, a broad PDS feature near 70 Hz is detected the low-hard state whereas a strong QPO feature is observed in the high-soft state (Trudolyubov 2000). In our interpretation, the oscillations in the near vicinity of the black hole are strongly smeared because they are viewed through a hot Compton cloud by the the observer. This prediction, based on the converging-inflow conceptual frame work should be confirmed or refuted by observations.

5. CONCLUSIONS

Based on a number of empirical trends in the literature regarding the temporal and spectral properties of BH binaries, supplemented by our own analysis of a number of these objects, we have presented a number of arguments in support of the BMC model. Most notably, the high-soft state spectral form, and the high frequency variability but long-term stability of the power law, which are problematic for thermal Comptonization scenarios, arise naturally in our model. These features, along with the other empirical trends such as the lack of temporal coherence between the soft and hard variability in the high-soft state, and increased coherence in the low-hard state further support our conjecture of the existence of a compact high-energy emission region located in the vicinity of BH horizon ($1 - 4R_S$). The total (kinetic) energy of the matter increases towards to the BH horizon. This radial gradient of the matter energy provides a natural explanation of the noted increase in QPO power with energy. A majority of efforts to explain these phenomena invoke thermal-Comptonizing media external to the disk. The problem with this approach, from our point of view, is that the physical parameters of the Comptonizing plasma require "fine tuning" to retain consistency with the ubiquitous nature of the spectral form. This is further compounded by the requirement to provide a self consistent explanation for the recently emerging temporal characteristics, such as this energy dependence of the high-frequency QPO power. If one for example, invokes radial thermal gradients to a Comptonizing plasma as an explanation of the QPO energy dependence, the inferred parameter space must be further tuned to allow one to consistently reproduce the emergent high-soft state spectral form over a considerable luminosity range.

Regarding the high-frequency QPOs, we predict analogous effects in AGN but with frequency rescaled in inverse proportion to BH mass, thus at least seven orders of magnitude lower, of order of 10^{-5} Hz. In particular, the narrow-line Seyfert-1 Galaxies which are characterized by the steep power law with $\alpha \sim 1.7$ and apparent soft excess emission, relative to the canonical $\alpha \sim 0.8$ X-ray spectra of the broader class of Seyfert-1 and quasar spectra. This may be related to mass-accretion rate (and thus to the host environment) in a manner similar to the bimodal spectral behavior of Galactic binaries, thus these objects would be the obvious candidates to search for this phenomenon. Nominal evidence for such oscillations has recently appeared in the literature (Boller, et al 2001).

We argue that the high-soft-state spectral form represents a unique black-hole event horizon signature. We further conjecture that an extra-Galactic analog may exist, namely the narrow line Seyfert-1 galactic nuclei. Given the ubiquitous nature of this phenomenon for many Galactic systems, and its apparent extension into the extra-Galactic realm, we suggest that we are witnessing a direct signature of the disappearance of matter falling down

the black-hole event-horizon drain.

ACKNOWLEDGMENTS

This work made use of the High-Energy Astrophysics Science Archive Research Center, the Compton Gamma Ray Observatory and Rossi X-Ray Timing Explorer science support facilities at the NASA Goddard Space Flight Center.

REFERENCES

- Barret, D., & Grindlay, J.E. 1995, *ApJ*, 440, 841
- Blandford, R.D., & Payne, D.G. 1981, *MNRAS*, 194, 1033
- Belloni, T et al. 1997, *A&A*, 322, 857
- Boller, T. et al. 2001, *A&A*, 365, L146
- Borozdin, K., Revnivtsev, M., Trudolyubov, S., Shrader, C.R., & Titarchuk, L.G. 1999, *ApJ*, 517, 367 (BOR99)
- Bottcher, M. & Liang, E.P. 2000, *ApJ*, submitted, astro-ph/0003139
- Burderi, L., Di Salvo, T., La Barbera, A., & Robba, N.R. 2001, *ApJ*, in press (astro-ph/0009183)
- Chakrabarti S.K. & Titarchuk, L. G. 1995, *ApJ*, 455, 623
- Chaty, S., et al. 2000, In proceeding of Integral workshop, Alicante, Spain
- Chen, W., Shrader, C.R., & Livio, M. 1997, *ApJ*, 491, 312
- Cheng, F.H., Horne, K., Panagia, N., Shrader, C.R., Gilmozi, R., Paresce, F., & Lund, N. 1992, *ApJ*, 397, 664
- Cui, W., Shrader, C.R., Haswell, C.A., & Hynes, R.I. 2000, *ApJ*, 535, L123
- Cui, W., Zhang, S.N., & Chen, W. 2000, *ApJ*, 531, L45
- Cui, W., Zhang, S. N., Focke, W., & Swank, J. H. 1997, *ApJ*, v.484, p.383
- Di Salvo, T., Stella, L., Robba, N.R., van der Klis, M., Burderi, L., Campana, S., Frontera, F., Israel, G.L., Homan, J. & Parmar, A.N. 2000, *ApJ*, 544, L119
- Dubus, G., Kim, R. S. J., Menou, K., Szkody, P. & Bowen, D. V. 2001, *ApJ*, 553, 307
- Focke, W., Swank, J., Philips, B., Heindl, W. & Cui, W. 1997, In proc. 4th Compton Symposium, AIP-CP410 (Eds. C.D. Dermer, M.S. Strickman, & J.D. Kurfess) 2, 854
- Gierlinski, M., Zdziarski, A.A, Poutanen, J., Coppi, P., Ebisawa, K. & Johnson, W. N. 1999, *MNRAS*, 309, 496.
- Grove, J.E., Johnson, W.N., Kroeger, R.A., McNaron-Brown, K., & Skibo, J.G. 1998, *ApJ*, 500, 899

- Grove, J.E. et al., 1997, In proc. 4th Compton Symposuim, AIP-CP410, (Eds. C.D. Dermer, M.S. Strickman & J.D. Kurfess) 1, 122
- Haswell, C.A., Skillman, D., Patterson, J., Hynes, R.I., & Cui, W. 2000, IAU, Ciril. 7427
- Heindl, M., & Smith, D.M. 1998, ApJ, 506, L35
- Homan, J., Wijnands, R., van der Klis, M., Belloni, T., van Paradijs, J., Klein-Wolt, M., Fender, R., & Mendez, M. 2001, ApJS, 132, 377
- Hua, X-M., & Titarchuk, L.G. 1995, ApJ, 449, 188
- Iaria, R., Burderi, L., Di Salvo, T., La Barbera, A., Robba, N.R. 2001, ApJ, 547, 412
- Laurent, Ph., & Titarchuk, L.G. 2001, ApJ, 562, L
- Laurent, Ph., & Titarchuk, L.G. 1999, ApJ, 511, 289 (LT99)
- Liang, E.P. 1998, Phys. Rep., 302, 66.
- Makishima, K., et al., 1986, ApJ, 308, 635
- Merloni, A., Fabian, A.C., & Ross, R.R. 2000, MNRAS, 313, 193
- McClintock, J.E., Garcia, M.R., Caldwell, N., Falco, E.E., Garnavich, P.M. & Zhao, P. 2001, ApJ, 551, L147
- Mitsuda, K., et al., 1984, PASJ, 36, 741
- Morgan, E.H., Remillard, R.A., Greiner, J., 1997, ApJ, 482, 993
- Nobili, L., Turolla, R., Zampieri, L., & Belloni, T. 2000, ApJ, 538, L137
- Nowak, M.A., Wilms, J., Heindl, W.A., Pottschmidt, K., Dove, J.B. & Begelman, M.C. 2001, MNRAS, 320, 327
- Papathanassiou, H., & Psaltis, D. 2001 MNRAS, submitted (astro-ph/0011447)
- Poutanen, J. & Svensson, R. 1996, ApJ, 470, 249
- Psaltis, D. 2001, ApJ, 555, 786
- Reig, P., Kylafis, N., & Spruit, H.C., 2001, A&A, 375, 155
- Remillard, R.A., McClintock, J.E., Sobczak, G.J., Bailyn, C.D., Orosz, J.A., Morgan, E.H., & Levine, A.M. 1999, 517, L127

- Shakura, N.I., & Sunyaev, R.A. 1973, *A&A*, 24, 337 (SS73)
- Shimura, T., & Takahara, F. 1995, *ApJ*, 445, 780
- Shrader, C.R., & Titarchuk, L.G. 1999, *ApJ*, 521, L121 (ShT99)
- Shrader, C.R., & Titarchuk, L.G. 1998, *ApJ*, 499, L31 (ShT98)
- Smith, D.A., Heindl, M., Markwardt, C.B., & Swank, J.H. 2001, *ApJ*, 554, L41
- Sobczak, G.J., McClintock, J.E., Remillard, R.A., Levine, A.M., Morgan, E.H., Bailyn, C.D., & Orosz, J.A. 1999, 517, L121
- Soria, R., Wu, K., Hannikainen, D., McCollough, M. & Hunstead, R. 2001, *A&A* submitted astro-ph/0108084
- Strickman, M., & Barret, D. 1999, In proc. of the fifth Compton Symposium, AIP-CP510 (Eds. M.L. McConnel and J.M. Ryan) p. 222
- Sunyaev, R.A., & Titarchuk, L.G. 1980, *A&A*, 86, 121
- Sunyaev, R.A., & Titarchuk, L.G. 1978, Preprint of the Space Research Institute of Soviet Academy of Science, 441.
- Sunyaev, R.A., & Trumper, J. 1979, *Nature*, 279, 506
- Titarchuk, L., & Osherovich, V. 2000a, *ApJ*, 537, L37 (T000a)
- Titarchuk, L., & Osherovich, V. 2000b, *ApJ*, 542, L111 (T000b)
- Titarchuk, L., & Osherovich, V. 1999, *ApJ*, 518, L95 (T099)
- Titarchuk, L., & Zannias, T. 1998, *ApJ*, 493, 863 (TZ98)
- Titarchuk, L. G., Mastichiadis, A., Kylafis, N. D. 1997, *ApJ*, 487, 834 (TMK)
- Titarchuk, L. G., Mastichiadis, A., Kylafis, N. D. 1996, *A&AS*, 120, C171
- Tomsick, J.A., Kaaret, P., Kroeger, R.A., & Remillard R.A. 1999, *ApJ*, 512, 892
- Tomsick, J. A., & Kaaret, Ph. 2001, *ApJ*, 548, 401 (astro-ph/0009354)
- Trudolyubov, S.P. 2001, *ApJ*, 558, 276
- Wood, K. S., Titarchuk, L.G., Ray, P.S, Wolf, M.T., Lovellete, M.N. & Bandyaopadhyay, R.M. 2001, *ApJ*, 563,

- Wood, K. S. et al. 2000, *ApJ*, 544, L45
- Zane, S., Turolla, R., Nobili, L., & Erna, M. 1996, *ApJ*, 466, 871
- Zdziarski, A. A., Grove, J.E., Poutanen, J., Rao, A.R., & Vadawale, S.V. 2001, *ApJ*, 554, L45 L45
- Zdziarski, A. 2000, *IAU Symposium* (Eds. P.C.H. Martens, S. Tsuruta & M.A. Weber), 195, p. 153 , v3, astro-ph/0001078
- Zhang, S.N., Cui, W., & Chen, W. 1997, *ApJ*, 482, L155
- Zhang, S.N., Cue, W., Chen, W., Yao, Y., Zhang, X., Sun, X., Wu, X-B., & Xu, H. 2000, *Science*, 287, 1239
- Zycki, P., Done, C., & Smith, D. 1998, *ApJ*, 496, L25.

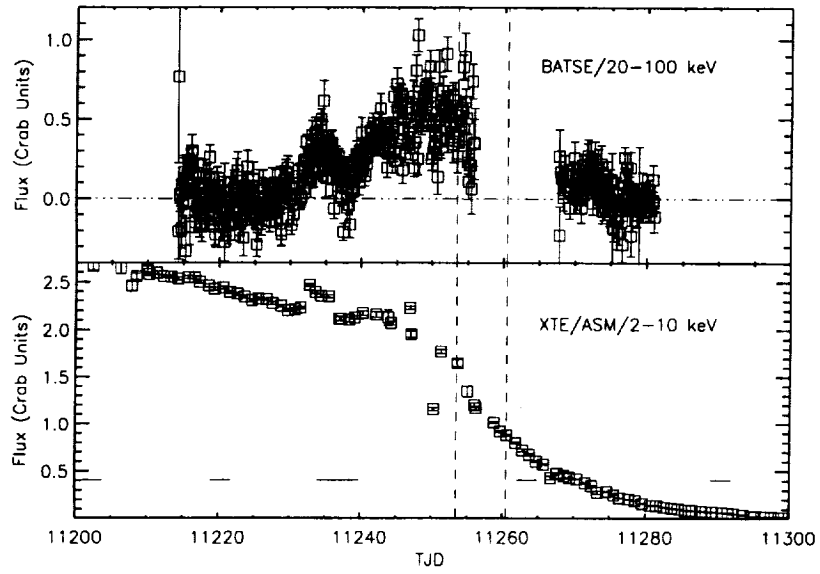


Fig. 1.— CGRO/BATSE and RXTE/ASM light curves covering the Spring 1999 active period of XTE J1550-564. The vertical, red, dashed lines indicate the VP 808.5 OSSE observation, and the short horizontal lines indicate pointed RXTE observations used in our analysis. The hard X-ray flux seems to be declining sharply during the OSSE observation (there is a gap in the BATSE coverage).

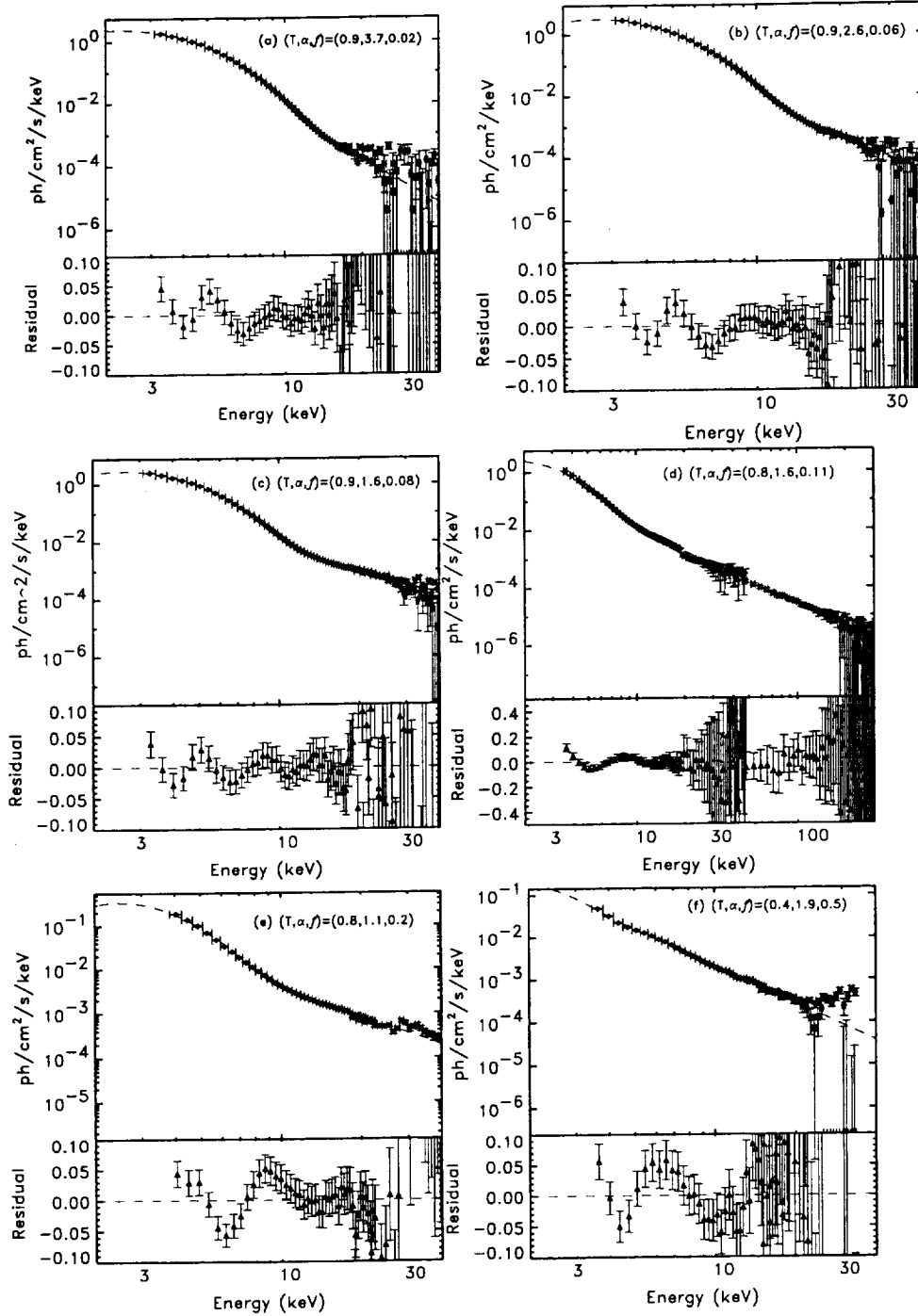


Fig. 2.— Evolution of the high-energy spectral energy distribution in XTE J1550-564. (a) represents the extreme high-soft state (about TJD 11220) when the hard-power law is marginal or absent. (b) is similar to (a) but the hard-power law is beginning to become more prominent. Panel (c) a transition to the more familiar high-soft state has occurred. Panel (d) is similar to (c). In panel (e) (TJD 11262) the luminosity has decreased significantly and the transition into the low-hard state is evident. In panel (f) (TJD 11293) is similar to (e).

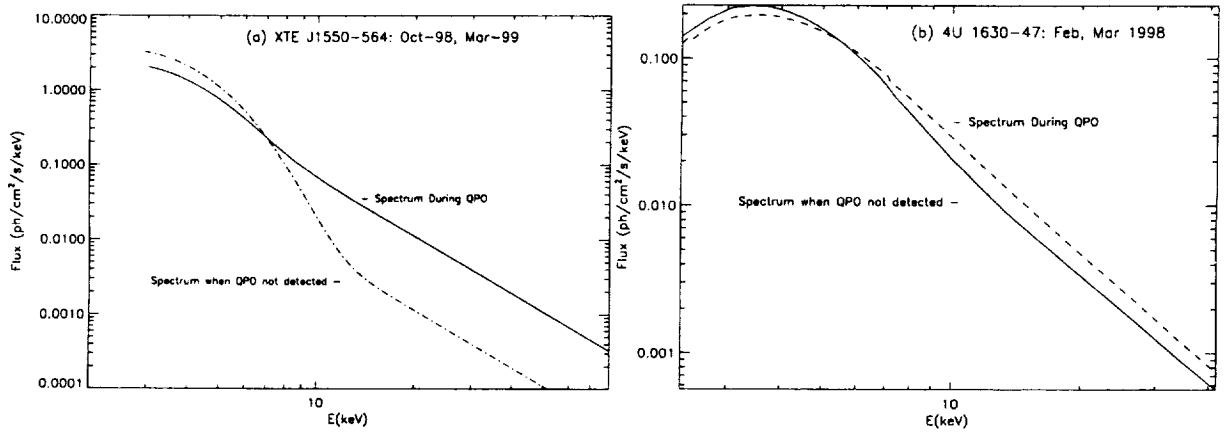


Fig. 3.— Continuum models fitted to the BHC X-ray nova (a) XTE J1550-564 at two epochs: October 1998 (solid curve), when 185-Hz QPOs were reported and March 1999 (dashed line) when no QPOs were observed. The relative normalization has been adjusted for illustrative purposes (the October 1998 case corresponds to higher flux state than March 1999). Note the distinctly different proportions of the hard - power law and soft thermal components. We interpret this as differences in the illumination geometry of the converging inflow site, parameterized by f in our model. Continuum models fitted to the BHC X-ray nova. In (b) similar, although less dramatic, effects are seen in 4U 1630-47 at two (QPO and non-QPO) epochs.

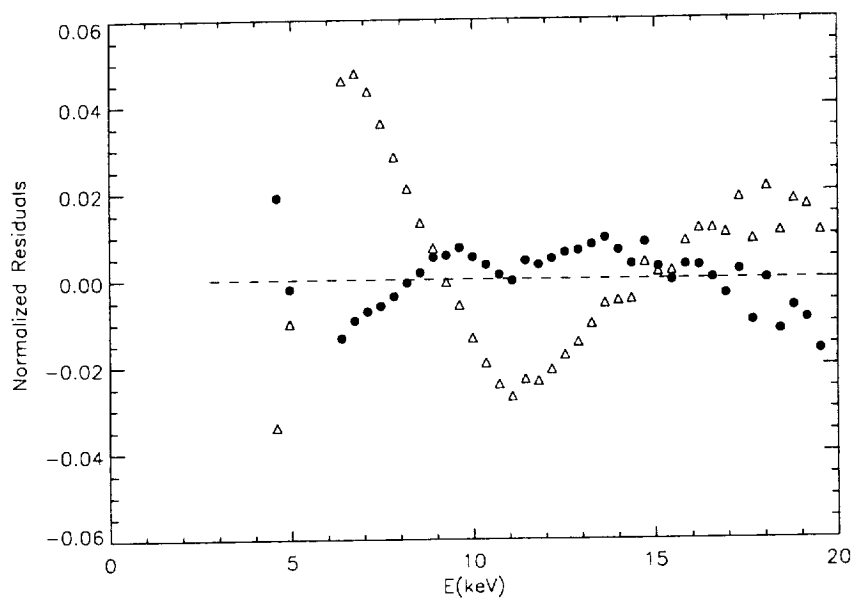


Fig. 4.— Normalized residuals (data minus model) for BMC (filled circles) and additive power law plus black-body disk (triangles). Note that while the BMC residuals are essentially contained within the several percent level, the additive model deviates significantly between 6 and 7 keV, and above about 15 keV. Such residuals could be misinterpreted as real spectral features.

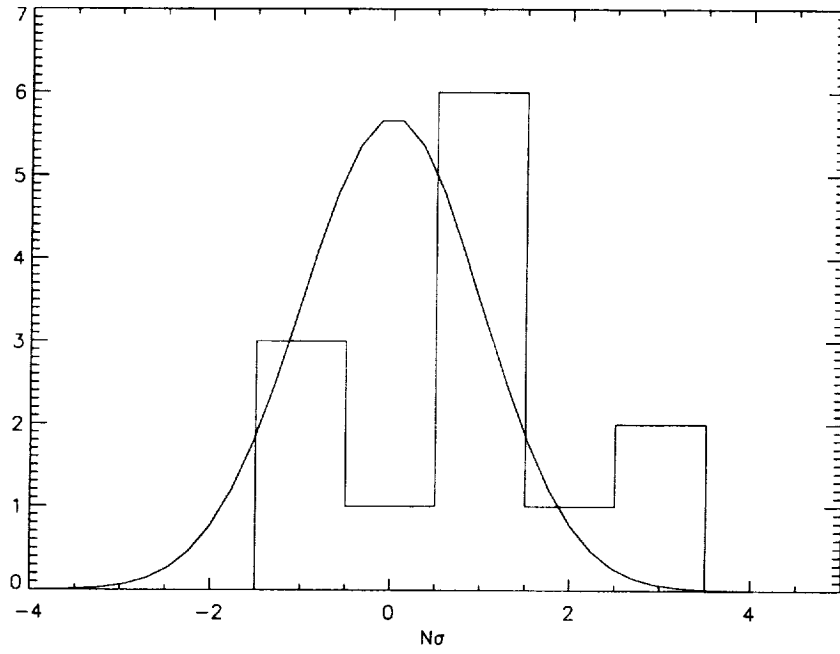


Fig. 5.— Statistical distribution of the $\sim 450\text{--}750$ keV detection significance resulting from our analysis of 14 spectra from 6 Galactic BH binaries observed with OSSE during the Compton GRO mission. The overlying curve, is a Gaussian with zero mean normalized to the data distribution.